Magnetic properties of $CaCu_3Ti_4O_{12}$: Fe solid solutions

Gavrilova Tatiana P.,[1*] Yagfarova Adilya R.,[1] Gilmutdinov Ildar F.,[1,2] Yatsyk Ivan V.,[1]
Deeva Julia A.,[3] Chupakhina Tatiana I.,[3] Vagizov Farit G.,[2] Eremina Rushana M.[1]

[1] Zavoisky Physical-Technical Institute, FRC Kazan Scientific Center of RAS, 420029, Kazan, Russia
[2] Institute of Physics, Kazan Federal University, 420008, Kazan, Russia
[3] Institute of Solid State Chemistry of RAS (UB), 620990, Ekaterinburg, Russia
** E-mail: tatyana.gavrilova@gmail.com*

Motivation

Calcium copper titanate $CaCu_3Ti_4O_{12}$ (CCTO) with the perovskite-type structure (space group $Im\bar{3}$, a = 7.391 Å [1, 2]) is already known as the giant dielectric permittivity material. CCTO has a high value of the dielectric constant $\varepsilon = 10^3 - 10^5$ and moderate dielectric loss (tan δ ~ 0.15) in a wide temperature range (40–450 K) for frequencies up to 10 MHz [3, 4, 5], that allows to use it in wide potential applications [6, 7, 8] as well as Fe-substituted CCTO [9].

The magnetic properties of the pure CCTO are also well known. It undergoes the phase transition into the antiferromagnetically ordered phase below T_N = 25 K with a Weiss constant of $\Theta_W \sim -30$ K, that was confirmed by some researchers through magnetometry, neutron scattering, Raman spectroscopy and electron spin resonance methods [11-12]. It is also known that the valence state of ions and magnetic properties of CCTO are sensitive to the doping or sample preparation process [13-17].

In this work, we present the thorough examinations of magnetic properties of $CaCu_{3-x}Ti_{4-y}Fe_{x+y}O_{12}$ (CCTO: Fe) solid solutions using Mössbauer spectroscopy, electron spin resonance and magnetometry methods, in order to reveal the relationship between the dopant concentration oxygen vacancies and magnetism in CCTO: Fe.

X-ray diffraction

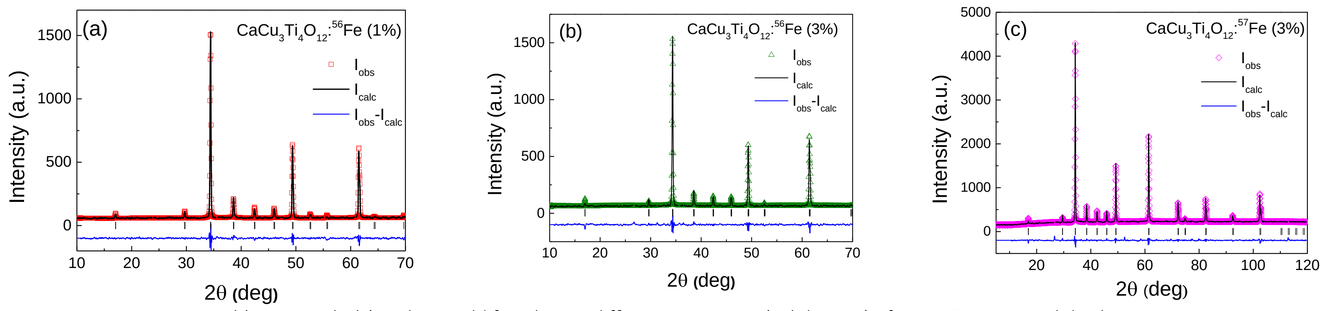

Fig. 1. Experimental (open symbols) and Rietveld fitted X-ray diffraction patterns (solid curve) of $CaCu_3Ti_4O_{12}$:Fe solid solutions at room temperature: (a) 1% ^{56}Fe, (b) 3% ^{56}Fe, (c) 3% ^{56}Fe+^{57}Fe. The residual difference is given in the bottom part of each panel

Table 1. Unit cell parameters for $CaCu_3Ti_4O_{12}$:Fe solid solutions; space group $Im\bar{3}$.

CCTO: Fe	a, Å	V, Å^3
0%	7.3906	
1% ^{56}Fe	7.3927	404.02
3% ^{56}Fe	7.3922	403.94
3% ^{57}Fe	7.3912	403.78

Decrease of ***a* lattice parameter** and **cell volume V** with increasing Fe concentration is due to:
(i) incorporation of Fe^{3+} ions in low spin state into Ti^{4+} octahedral positions (Fig.2a)
(ii) incorporation of Fe^{3+} ions into Cu^{2+} planar positions (Fig.2b)
(iii) presence of Fe^{2+} ions

Mossbauer spectroscopy

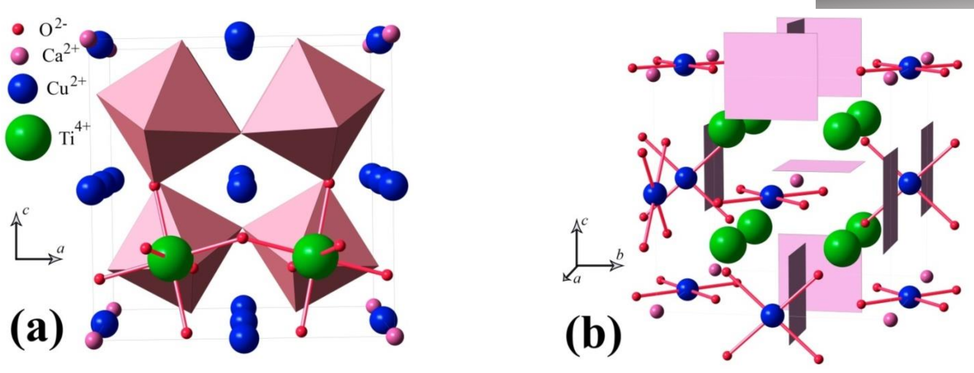

Fig. 2. Crystal structure of calcium copper titanate $CaCu_3Ti_4O_{12}$: (a) octahedral Ti^{4+} positions, (b) planar Cu^{2+} positions.

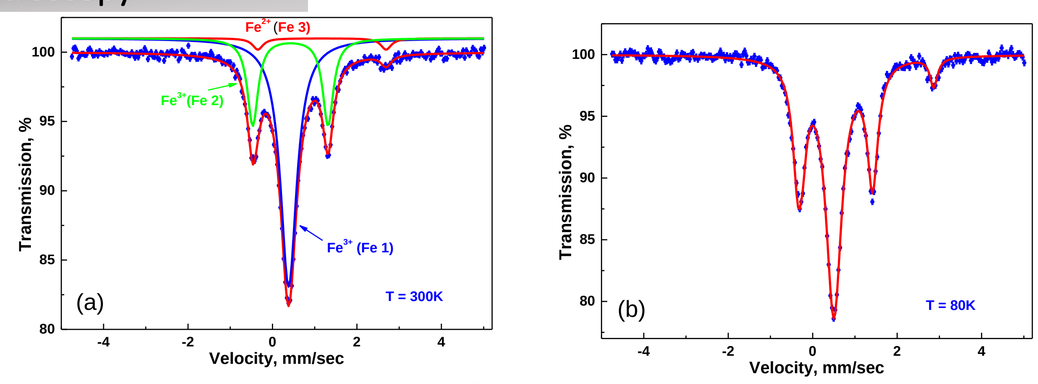

Fig. 3. Mossbauer spectra of $CaCu_3Ti_4O_{12}$:^{56}Fe+^{57}Fe (3%) sample at different temperatures: (a) T = 300K and (b) T = 80 K.

Table 2. Mössbauer hyperfine parameters of the components of the $CaCu_3Ti_4O_{12}$:Fe (1, 3%) solid solutions measured at RT.

	Fe^{3+} (Fe 1)				Fe^{2+} (Fe 3)				Fe^{3+} (Fe 2)				
	δ, mm/s	QS, mm/s	W, mm/s	A,%	δ, mm/s	QS, mm/s	W, mm/s	A,%	δ, mm/s	QS, mm/s	W, mm/s	A,%	χ^2
1% ^{56}Fe	0.36	0.09	0.29	55	1.00	3.13	0.29	28	0.40	1.70	0.26	17	0.70
3% ^{56}Fe	0.35	0.05	0.33	56	1.12	2.94	0.39	15	0.38	1.73	0.29	29	0.89
3% ^{57}Fe	0.382	0.038	0.460	65.5	1.17	3.04	0.30	3.9	0.425	1.783	0.307	30.6	0.87

Based on Mossbauer spectroscopy data one can conclude that Fe ions substitute Ti^{4+} and Cu^{2+} positions in octahedral (Fig.2a) and planar (Fig.2b) oxygen environment, respectively. Such type of substitution leads to the appearance of three types of iron magnetic centers: divalent Fe^{2+} planar (**Fe2**) and trivalent Fe^{3+} in symmetrical (**Fe1**) and distorted (**Fe3**) octahedral positions.

Magnetization measurements

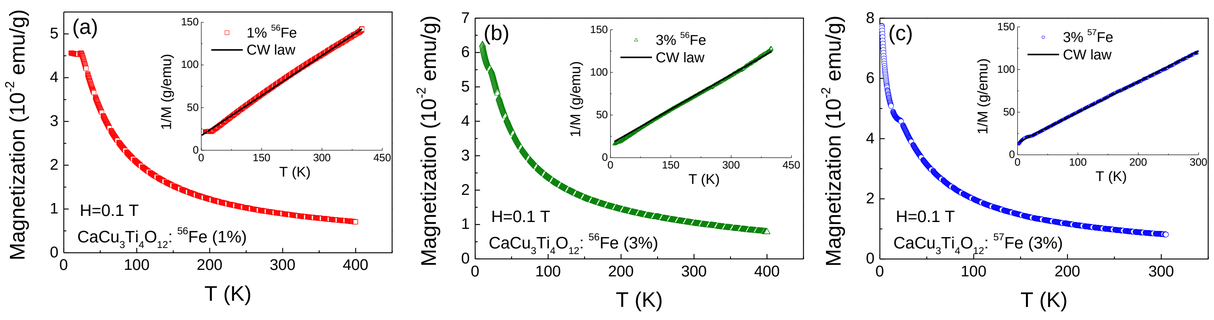

Fig. 4. Temperature dependence of magnetization of $CaCu_3Ti_4O_{12}$:Fe solid solutions: (a) 1% ^{56}Fe, (b) 3% ^{56}Fe, (c) 3% ^{57}Fe measured in FC regime in the external magnetic field H = 0.1 T. Insets show the inverse magnetization as a function of temperature.

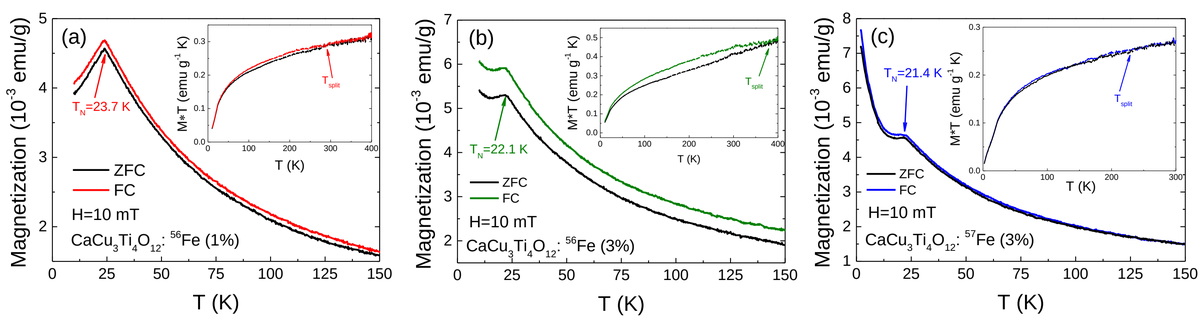

Fig. 5. Temperature dependence of magnetization of $CaCu_3Ti_4O_{12}$:Fe solid solutions: (a) 1% ^{56}Fe, (b) 3% ^{56}Fe, (c) 3% ^{57}Fe measured in FC and ZFC regimes in the external magnetic field H = 10 mT. Insets show the same data in representation M·T vs. T.

Table 3. Fitting parameters of the temperature dependence of the magnetization measured in FC regime in the external magnetic field H = 0.1T in $CaCu_3Ti_4O_{12}$: Fe (1, 3%) solid solutions.

Sample	0%	1% ^{56}Fe	3% ^{56}Fe	3% ^{57}Fe
Néel temperature T_N (K)	25[10, 12]; 24.1 [11]	23.7	22.1	21.4
Curie constant C (emu·K·mol^{-1}·Oe^{-1})	1.41 [12]	1.97	2.28	1.72
Weis constant Θ_{CW} (K)	-30 [10]; -32.6 [18]	-55	-60	-40
Effective magnetic moment μ_{eff} (μ_B)	3.36 [12]	3.97	4.27	3.71
ZFC-FC splitting temperature T_{split} (K)	-	290	380	230

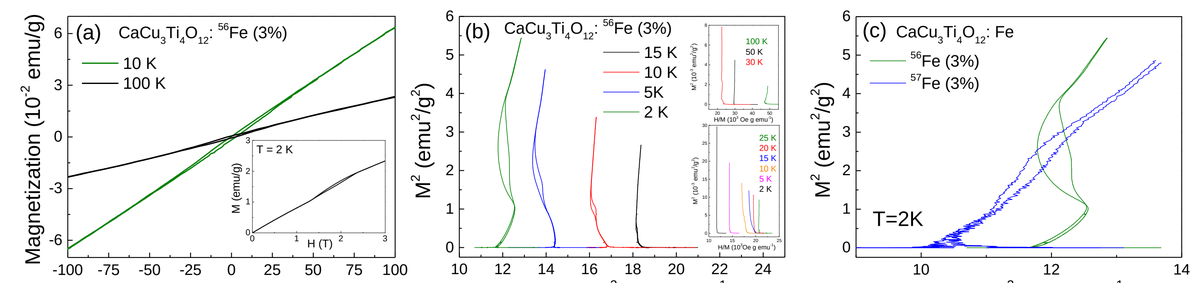

Fig. 6. (a) Magnetization as a function of the external magnetic field in $CaCu_3Ti_4O_{12}$:^{56}Fe (3%) solid solution, measured at temperatures of 10 K and 100 K. Inset the M-H curve measured at T=2 K in the range of the magnetic fields up to 3 T.
(b) Arrott plots below the magnetic phase transition temperature in $CaCu_3Ti_4O_{12}$:^{56}Fe (3%) solid solution in the range of magnetic field up to 3 Tesla. Insets show the Arrott plot near the magnetic phase transition temperature. (c) Arrott plots at T = 2K in $CaCu_3Ti_4O_{12}$:Fe solid solutions in the range of magnetic field up to 3 Tesla.

Most interesting magnetic properties including the metamagnetic phase transitions (Fig. 6), the significant ZFC-FC splitting (Fig. 4) and the highest value of the Weis constant (Table 3), are observed in $CaCu_3Ti_4O_{12}$:^{56}Fe (3%) sample where both the essential amount of Fe^{3+} ions in distorted octahedral position together with Fe^{2+} are present (Table 2).

Electron spin resonance

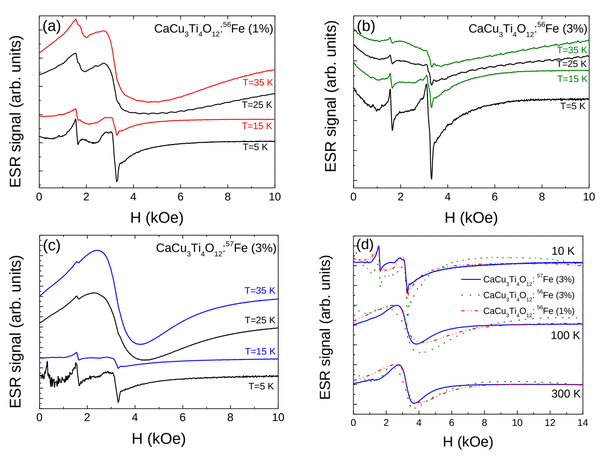

Fig. 7. Typical electron spin resonance spectra below the Néel temperature in $CaCu_3Ti_4O_{12}$:Fe solid solutions: (a) 1% ^{56}Fe, (b) 3% ^{56}Fe, (c) 3% ^{57}Fe.
(d) Comparative view of the ESR spectra for $CaCu_3Ti_4O_{12}$:Fe at different temperatures.

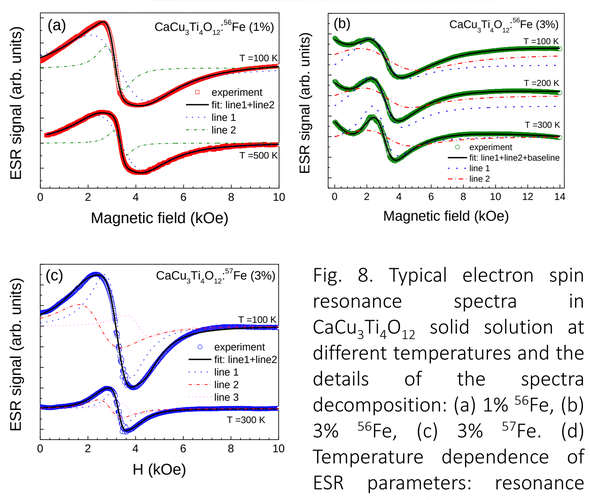

Fig. 8. Typical electron spin resonance spectra in $CaCu_3Ti_4O_{12}$ solid solution at different temperatures and the details of the spectra decomposition: (a) 1% ^{56}Fe, (b) 3% ^{56}Fe, (c) 3% ^{57}Fe. (d) Temperature dependence of ESR parameters: resonance field, linewidth, normalized integral intensity.

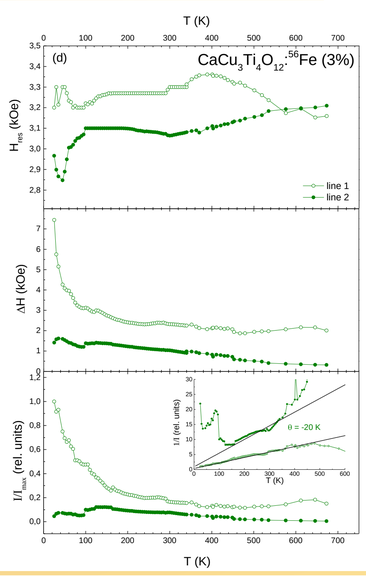

At low temperatures $T < T_N$ the paramagnetic phase in CCTO:Fe goes into magnetically ordered state (canted antiferromagnetic or ferrimagnetic state), that confirms by the significant drop in the integral intensity (Fig. 7). Above the magnetic phase transition temperature the observed ESR absorption samples is well described by the sum of two field derivative of a Lorentz line (Fig. 8a, b, c). We suggest that the both lines (dependencies with indexes 1 and 2) are signals from paramagnetic phases. The Weiss constants which was obtained from the fitting of the ESR integral intensity (f.e. inset in parts d in Fig. 8) is equal to θ = -6 K, -20 K and 10 K for $CaCu_3Ti_4O_{12}$ doped with ^{56}Fe (1%), ^{56}Fe (3%) and ^{57}Fe (3%), respectively; that coincides in the changes dynamics of Weiss constants from the magnetization measurements (Table 3).

[1] E.S. Božin, et al. J. Phys.:Condens. Matter 16 (2004) S5091–S5102
[2] B. Bochu, et al. J. Solid State Chem. 29 (1979) 291–298
[3] M.A. Subramanian, et al. J. Solid State Chem. 151 (2000) 323–325
[4] P. Lunkenheimer, et al. Eur. Phys. J. Spec. Top. 180 (2009) 61–89
[5] U. M. Meshiya, et al. Vib. Spectroscopy 112 (2021) 103201 1 – 9
[6] R. Löhnert, et al. J. Am. Ceram. Soc. 98 (2014) 141–147
[7] L.C. Kretly, et al. Microw. Opt. Technol. Lett. 39 (2003) 145–150
[8] M.A. Ponce, et al. J. Eur. Ceram. Soc. 35 (2015) 153–161
[9] K. Pal, et al. Chemical Physics Letters 709 (2018) 110–115
[10] A. Koitzsch, et al. Phys. Rev. B 65 (2002) 052406 1–4
[11] Y. Kim, et al. Solid State Commun., 121 (2002) 625-629
[12] M. Pires, et al. Phys. Rev. B, 73 (2006) 224404 1 – 7
[13] J.F. Fernandez, et al. J. Am. Ceram. Soc., 92 (2009) 2311-2318
[14] P. Pansara, et al. Phys. Chem. Chem. Phys., 20 (2018) 1914-1922
[15] P. Raval, et al. Ceram. Int., 44 (2018) 17667-17674
[16] U. M. Meshiya, et al. Ceramics International 46 (2020) 2147–2154
[17] P. Y. Raval, et al. J Mater Sci: Mater Electron (2021) 32:13630–13638
[18] Y. Shimakawa, T. Saito. Phys. Status Solidi B 249 (2012) 423–434